Production of η' from thermal gluon fusion

Sangyong Jeon
Department of Physics, McGill University, 3600 University Street, Montreal, Québec, Canada H3A 2T8
and RIKEN-BNL Research Center, Brookhaven National Laboratory, Upton, New York 11973
(Received 26 July 2001; published 11 January 2002)

We study the production of η' from hadronizing thermal gluons using recently proposed η'-g-g effective vertex. The η' yield is found to be sensitive to the initial condition. At RHIC and LHC, the enhancement is large enough to be easily detected.

DOI: 10.1103/PhysRevC.65.024903 PACS number(s): 25.75.Dw, 24.10.Pa

I. INTRODUCTION

If the hadronic Lagrangian is symmetric under flavor U(3) which is spontaneously broken, then we would have nine pseudoscalar Goldstone bosons. In reality, we have eight light mesons (π, K, η) corresponding to the octet of SU(3) and one heavy meson η'.

The pseudoscalar flavor singlet η' is a remarkable resonance. Its large mass poses the $U_A(1)$ problem and its possible resolution relates its mass to the topological charge of the QCD vacuum and to the properties of the instanton liquid [1–4].

In heavy ion physics, the η' meson is a good probe because it has a lifetime (1000 fm) long compared to the typical lifetime of a fireball produced by a collision of relativistic heavy ions. This was exploited by the authors of Ref. [5] who studied possible lowering of the η' mass by the disappearance of the instanton liquid at high temperatures. In it, the authors argued that even in dense matter the η' meson may decouple from the rest of the matter.

Recently, there was a surge of interest in η' in the study of *B*-meson decays and search for new physics [6–10]. In some of these studies, the axial anomaly relation

$$\partial^\mu J^0_{5\mu} = 2N_f \frac{g^2}{16\pi^2} \mathrm{Tr}(G_{\mu\nu}\tilde{G}^{\mu\nu}) \tag{1.1}$$

is interpreted to imply that the gluons and η' have an effective Wess-Zumino-Witten–type interaction vertex [7,10] (see also [11]),

$$M_{\lambda\gamma}\delta^{ab} = H(p^2,q^2,P^2)\,\delta^{ab}\epsilon_{\mu\nu\alpha\beta}p^\mu q^\nu (\epsilon_p^\alpha)_\lambda (\epsilon_q^\beta)_\gamma, \tag{1.2}$$

where p,q are the gluon momenta and $(\epsilon_{p,q})_{\lambda,\gamma}$ are the corresponding gluon polarization vectors and the superscripts ab denote the color indices of the two gluons. The momentum of η' is denoted by P throughout the paper. By studying $J/\psi \to \eta'\gamma$ decay process, Atwood and Soni [7] found that this process is dominated by on-shell gluons and obtained

$$H_0 \equiv H(0,0,M^2_{\eta'}) \approx 1.8\ \ \mathrm{GeV}^{-1}. \tag{1.3}$$

The above $gg\eta'$ effective vertex is interesting in many ways. First, since the η' mass is almost 1 GeV, at least one of the gluon momenta involved in the vertex should be greater than 0.5 GeV. Therefore the gluon momenta are not soft compared to the temperatures achievable in heavy ion collisions. Second, this is a rare occasion when we know (at least we can parametrize) how to fuse two on-shell gluons and form a hadron. There are models in the literature that relate *constituent* quarks to the hadrons, but to the author's knowledge, there is no other known matrix element between gluons and a known hadron state.

In this paper, we exploit these unique circumstances and study the production of the η' mesons from the hadronizing quark-gluon plasma. One question we have to answer before we proceed is how the interaction strength $H_0 = H(0,0,M^2_{\eta'})$ changes as the temperature increases. To fully answer this question, one has to evaluate the triangle diagram which gives rise to Eq. (1.1) using an effective field theory at finite temperature. Evaluation of such a diagram at zero temperature has been carried out by Muta and Yang [12]. However, the finite-temperature calculation is still to be performed. In this work, we will simply take the coupling to be the same as the vacuum value, $H_0 = 1.8\ \ \mathrm{GeV}^{-1}$. Work on the finite-temperature correction is currently in progress.

One can, however, make an interesting observation from the works on the finite-temperature modification of $\pi^0\gamma\gamma$ coupling. This is relevant because both π^0 and η' are pseudoscalars and both γ and g are vectors. Therefore the structure of the triangle diagram underlying Eq. (1.1) (cf. Ref. [12]) is very similar to the triangle diagram that gives rise to $\pi^0\gamma\gamma$ coupling. In Ref. [13], it is shown that the $\pi^0\gamma\gamma$ vertex vanishes as the temperature approaches the chiral symmetry restoration temperature even though the axial anomaly itself remains nonvanishing [15–17]. The authors also anticipated that a similar modification should be relevant for $\eta' gg$ coupling. One would not, however, expect $\eta' gg$ coupling to vanish in this limit because η' is not a Goldstone boson. The authors of Ref. [14] carefully analyzed the triangle diagram at finite temperature and obtained

$$g_{\pi\gamma\gamma} = \frac{m_q}{T^2} e^2 g_{\pi q\bar{q}} \mathcal{F}[g_{\pi q\bar{q}}, \alpha, \alpha \ln 1/e, \ldots], \tag{1.4}$$

where m_q is the constituent quark mass, e is the electromagnetic coupling constant, and $g_{\pi q\bar{q}}$ is the π^0-quark-antiquark coupling constant. $\mathcal{F}$ is a finite function of coupling constants. The vanishing of $\pi^0\gamma\gamma$ coupling is then attributed to the vanishing of the constituent u and d quark masses near T_c.

Since the triangle diagrams are similar, we can borrow the above expression to roughly estimate the $\eta' gg$ coupling constant at nonzero T to be

$$g_{\eta' gg} = H_0 \sim \frac{m_q}{T^2}, \tag{1.5}$$

where all other factors in this case should be $O(1)$. Near T_c, the u and d quark masses vanish. However, the strange quark mass does not vanish. Since $\eta' \approx (u\bar{u} + d\bar{d} + s\bar{s})/\sqrt{3}$, this indicates that the $\eta' gg$ vertex remains finite near T_c. Furthermore, $g_{\eta' gg}$ is proportional to the strange quark mass. This in turn enables us to observe that the η' mesons so produced near T_c will be dominated by $s\bar{s}$ component (cf. Ref. [5]).

There is no doubt that to do a more quantitative calculation, we need to calculate the $\eta' gg$ vertex at finite-temperature with full finite temperature complications. In this work, we take a constant $H_T = 1.8\ \mathrm{GeV}^{-1}$ but take η' from gluon fusion to be in the $s\bar{s}$ state so that $M_{\eta'} \approx 0.7$ GeV [5].

II. KINETIC THEORY APPROACH

Kinetic equations are a statement about the change of the phase space density in time:

$$\frac{df}{dt} = (\text{gain rate}) - (\text{loss rate}). \tag{2.1}$$

To write down a Boltzmann equation for η' distribution function, it is easiest to start with the decay rate. In terms of the matrix element, the decay rate of η' to two gluons of the opposite colors and different polarizations is given by

$$d\omega_{\eta' \to gg} = \delta^{ab} \frac{1}{2} \frac{1}{2E_P} |M_{\lambda\gamma}|^2 \frac{d^3p}{(2\pi)^3 2p} \frac{d^3q}{(2\pi)^3 2q} \times (2\pi)^4 \delta^4(p+q-P), \tag{2.2}$$

where p and q are the gluon momenta and P is the η' momentum. The first factor of 1/2 is the symmetry factor. Summing over all final states gives the total decay rate. It is then convenient to define

$$|M|^2_{\eta' \to gg} = \sum_{ab} \delta^{ab} \sum_{\lambda,\gamma} |M_{\lambda\gamma}|^2. \tag{2.3}$$

It is not hard to show

$$|M|^2_{\eta' \to gg} = 4|H_0|^2 M^4_{\eta'} \tag{2.4}$$

using the identities

$$\sum_{\lambda} (\epsilon^{\alpha}_p)^*_{\lambda} (\epsilon^{\zeta}_p)_{\lambda} = -g^{\alpha\zeta} + ap^{\alpha}p^{\zeta}, \tag{2.5}$$

$$\epsilon_{\alpha\beta\mu\nu} \epsilon^{\alpha\beta\rho\sigma} = 2(g^{\mu}_{\sigma} g^{\nu}_{\rho} - g^{\mu}_{\rho} g^{\nu}_{\sigma}), \tag{2.6}$$

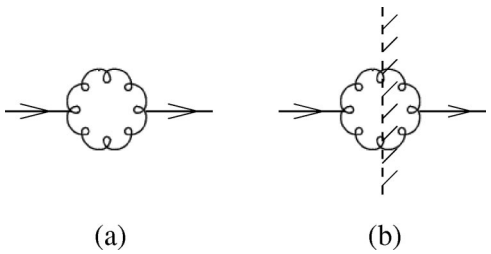

(a) (b)

FIG. 1. Feynman graphs for the retarded self-energy of η'.

and the on-shell conditions $p^2 = q^2 = 0$ and $(p+q)^2 = M^2_{\eta'}$. The $ap^{\alpha}p^{\zeta}$ term in Eq. (2.5) does not contribute to $M_{\lambda\gamma}$ due to the antisymmetric property of $\epsilon_{\alpha\beta\mu\nu}$.

Employing the principle of detailed balance, we then write the Boltzmann equation for the phase space density of η' as

$$\begin{aligned} &\partial_t f_{\eta'}(P) + \mathbf{v} \cdot \nabla f_{\eta'}(P) \\ &\quad = \frac{1}{2} \frac{1}{2E_P} \int \frac{d^3p}{(2\pi)^3 2p} \frac{d^3q}{(2\pi)^3 2q} \\ &\qquad \times (2\pi)^4 \delta(p+q-P) |M|^2_{gg \to \eta'} \{ f_g(p) f_g(q) \\ &\qquad \times [1 + f_{\eta'}(P)] - [1 + f_g(p)][1 + f_g(q)] f_{\eta'}(P) \}, \end{aligned} \tag{2.7}$$

where $\mathbf{v} = \mathbf{P}/E_P$. Here it is understood that the distribution functions depend on the space-time. In the Boltzmann equation, the first term in the collision integral describes the production of η' from the gluons and the second term describes the decay of η' into two gluons. These collision terms are essentially the imaginary part of the retarded self-energy of η' [18] depicted in Fig. 1(b).

In a series of papers [18,19], it was shown that in a thermal medium, the real part of the self-energy must be also included in the mass parameter appearing in the Boltzmann equation. With the effective vertex, Eq. (1.2), one can easily calculate the one-loop self-energy represented by the Feynman diagrams in Fig. 1. The details of their evaluation are presented in Appendix A. In the present case, it turned out that the thermal correction is negligibly small up to $T \approx 0.5$ GeV. Therefore we can safely ignore it for our purposes.

Before proceeding to analyze the Boltzmann equation, we must ask if we can use the Boltzmann equation in a quark gluon plasma. In other words, can η' exist in a quark gluon plasma as a quasiparticle? It is possible that an excitation with the same quantum numbers as η' can exist in the plasma (for instance, see [5]) but its width may be too broad to be a quasiparticle. To be conservative, we apply the Boltzmann equation starting only from one relaxation time before the hadronization time unless the hadronization time is shorter than the relaxation time.

If the steady state is reached during the evolution, then the Boltzmann equation dictates that distribution functions become Bose-Einstein functions. In this case, the distribution of η' at the hadronization time will be simply the Bose-

Einstein distribution with a temperature of $T_c \approx 0.17$ GeV. This in itself is an interesting conclusion because there are surely other hadronization processes and hadronic processes that produce additional η'. Since the η' lifetime is about 1000 fm and the mean free path in dense hadronic matter exceeds 10 fm [5], the final η' multiplicity will exceed thermal model expectation.

However, local chemical equilibrium between η' and gluons may not be readily reached during the quark-gluon plasma evolution although quarks and gluons do reach local equilibrium very fast. Therefore, $f_{\eta'}$ must evolve nontrivially in time even if the gluons are already locally equilibrated. To calculate such an effect, we assume that the gluon density is already thermal and rewrite the above as

$$\begin{aligned}\partial_t f_{\eta'} + \mathbf{v}\cdot\nabla f_{\eta'} &= \frac{1}{4E_P}\int \frac{d^3p}{(2\pi)^3 2p}\frac{d^3q}{(2\pi)^3 2q}|M|^2_{gg\to\eta'} \\ &\times (2\pi)^4\delta(p+q-P)\times f_g(p) f_g(q) \\ &\times [1 - f_{\eta'}(P)/f_{BE}(P)], \end{aligned} \tag{2.8}$$

where $f_{BE}(P) = 1/(e^{E_P/T}-1)$. Substituting the matrix element yields

$$\partial_t f_{\eta'} + \mathbf{v}\cdot\nabla f_{\eta'} = \frac{|H_0|^2 M^4_{\eta'}}{E_P}[1 - f_{\eta'}(P)/f_{BE}(P)]\Gamma_2(P), \tag{2.9}$$

where the two-body thermal phase space factor is given by

$$\begin{aligned}\Gamma_2(P) = \int \frac{d^3p}{(2\pi)^3 2p}\frac{d^3q}{(2\pi)^3 2q}(2\pi)^4 \\ \times \delta(p+q-P) f_g(p) f_g(q). \end{aligned} \tag{2.10}$$

The evaluation of $\Gamma_2(P)$ can be found in Appendix B. In the Boltzmann limit,

$$\Gamma_2(P) = \frac{1}{8\pi} e^{-E_P/T}. \tag{2.11}$$

For simplicity, we take the Boltzmann limit from now on. As for the gluon evolution, we use hydrodynamic models with one-dimensional (1D) expansion to make a simple physical estimate. In terms of the space-time rapidity $\eta = (1/2)\ln[(t+z)/(t-z)]$, the flow velocity in the 1D Bjorken model is given by

$$u^\mu = (\cosh\eta, 0, 0, \sinh\eta). \tag{2.12}$$

Using the ideal gas equation of motion $\epsilon = 3p$ results in a simple time dependence of the temperature

$$T(\tau) = T_0\left(\frac{\tau_0}{\tau}\right)^{1/3}, \tag{2.13}$$

where $\tau = \sqrt{t^2 - z^2}$ is the proper time and T_0 is the temperature at the initial (proper) time τ_0. Further, we limit the η' momenta to be at the central rapidity so that $v_z = P_z/E_P = 0$. In that case, only the time derivative term from the left-hand side of the Boltzmann equation remains nonvanishing. The coordinate z and the momentum P merely are parameters in 1D ordinary differential equation

$$\frac{df(t,z,P)}{dt} = \frac{|H_0|^2 M^4_{\eta'}}{8\pi E_P}[e^{-E_P \cosh\eta/T(\tau)} - f(t,z,P)], \tag{2.14}$$

where we have omitted the subscript label η' from the distribution and η and T are functions of t and z. This is in the form of a relaxation equation. The relaxation time is given by

$$t_P^{\rm rel} = \frac{8\pi E_P}{|H_0|^2 M^4_{\eta'}} = \tau_{\rm rel}\gamma_P, \tag{2.15}$$

where $\tau_{\rm rel} = 4.5$ fm is the relaxation time in the rest frame of the η' and $\gamma_P = E_P/M_{\eta'}$ is the Lorentz γ factor associated with the η' momentum. Here we used $M_{\eta'} = 0.7$ GeV in accordance with our earlier discussion. Up to the momentum of 1 GeV, the typical γ factor does not exceed 2. Therefore the relaxation time is comparable with the typical plasma lifetime of 1–10 fm. The relaxation time $t_P^{\rm rel}$ is independent of the temperature unless H_0 and/or $M_{\eta'}$ depends strongly on T.

The solution of the above equation is given by

$$f(t,z,P) = \int_{t_{\rm init}}^{t} \frac{dt'}{t_P^{\rm rel}} e^{-(t-t')/t_P^{\rm rel}} f_0(t',z,P), \tag{2.16}$$

with the initial condition $f(t_{\rm init},z,P) = 0$ and $f_0(t',z,P) = e^{-E_P\cosh\eta(t',z)/T(t',z)}$. What we are interested in is the distribution function at the hadronization time $t_{\rm had}$. In the Bjorken model, the proper time at the hadronization is given by

$$\tau_{\rm had} = \tau_0\left(\frac{T_0}{T_c}\right)^3. \tag{2.17}$$

We then take the initial proper time for the η' evolution to be the larger of τ_0 and

$$\tau_{\rm init} = \tau_{\rm had} - \tau_{\rm rel}. \tag{2.18}$$

The Mikowskian time and the proper time is related by

$$t = \sqrt{\tau^2 + z^2}. \tag{2.19}$$

Therefore, the farther away from the origin, the later the initial time is. This is due to the strong longitudinal flow and time dilation associated with it. The longitudinal flow is faster farther away from the origin. It also means that at large z, there will be very little time between the onset of η' production by fusing gluons and the hadronization time.

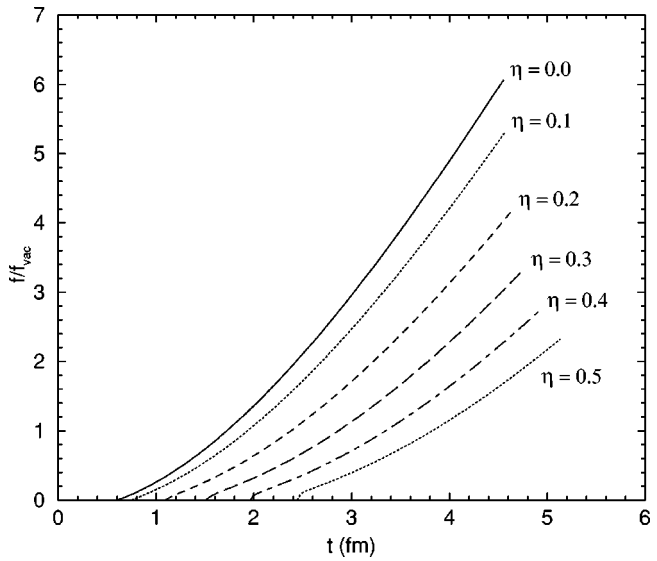

FIG. 2. The ratio of the solution of Eq. (2.16) and $f_0 = e^{-M_0 \cosh \eta(t,z)/T(t,z)}$ at $P=0$ as a function of time. Here $M_0 = 0.958$ GeV is the vacuum η' mass. From the bottom, the curves correspond to the *final* space-time rapidities $\eta = 0.0$–0.5 in steps of 0.1 at $t_{\rm had}$. Calculated with the RHIC parameters. The end points correspond to $t_{\rm init} = \sqrt{\tau_{\rm init}^2 + z^2}$ and $t_{\rm fin} = \sqrt{\tau_{\rm fin}^2 + z^2}$.

III. NUMERICAL RESULTS

To evaluate Eq. (2.16), we take $T_0 = 0.334$ GeV and $\tau_0 = 0.6$ fm. These parameters are taken from a recent hydrodynamic study of the elliptic flow at RHIC [20]. The initial temperature corresponds to the average energy density of about 23 GeV/fm^{-3}. The hadronization proper time with these parameters is $\tau_{\rm had} = 4.6$ fm. Since $\tau_{\rm had} - \tau_{\rm rel} = 0.1$ fm is shorter than τ_0, we set $\tau_{\rm init} = \tau_0$.

Figure 2 shows the numerical solutions with $P=0$ within the time interval $t_{\rm init} \leqslant t \leqslant t_{\rm had}$. In Fig. 2 we plot the ratio of our solution and what one expects from the thermal model,

$$f_{\rm vac} \equiv \exp[-M_0 \cosh \eta(t,z)/T(t,z)], \tag{3.1}$$

where M_0 is the mass of η' in vacuum.

The curves in Fig. 2 start from zero and keep growing. This is due to two reasons. One, the solution itself overshoots the equilibrium distribution f_0 (which has the same in-medium $M_{\eta'} = 0.7$ GeV) because the temperature is a decreasing function of time. Initially the slope df/dt is too steep for the eventual temperature of $T_c = 0.17$ GeV. Two, since the in-medium mass is 30% smaller than the vacuum mass, $f_{\rm vac}$ in Eq. (3.1) decreases much faster than either f or f_0 as t increases.

It is also apparent that for larger η or equivalently larger z, there is not enough time between $t_{\rm init} = \sqrt{\tau_{\rm init}^2 + z^2}$ and $t_{\rm fin} = \sqrt{\tau_{\rm fin}^2 + z^2}$ for the solution to grow over $f_{\rm vac}$. Consequently, the enhancement of $dN_{\eta'}/dy$ at the midrapidity ($y=0$),

$$\frac{(dN_{\eta'}/dy)_f}{(dN_{\eta'}/dy)_{f_{\rm vac}}} \approx 2.5 \quad \text{(RHIC)}, \tag{3.2}$$

is not as large as the enhancement of f at $\eta = 0$. Here we used

$$\frac{dN_{\eta'}}{dy}\Big|_{y=0} = \int \frac{d^2P_T}{(2\pi)^3} E_P \int d^3x f(t_{\rm had}, z, P_T). \tag{3.3}$$

This enhancement factor is not particularly sensitive to the initial temperature. Keeping τ_0 fixed, the ratio is 1.8 at $T_0 = 0.3$ GeV, increases up to 2.6 at $T_0 = 0.35$ GeV, and then decreases to 2.2 at $T_0 = 0.4$ GeV.

One should note that this is *on top* of other processes that produce η' at the hadronization and in later times. Therefore, this result definitely indicates a large enhancement in the η' yield due to the thermal gluon fusion process at RHIC.

At LHC, the initial temperature can reach $T_0 = 1$ GeV. Accordingly, the hadronization takes place much later, $\tau_{\rm had} = 10$–20 fm, even though the equilibration time is shorter, $\tau_0 \approx 0.1$ fm [21]. Therefore the rate of the change in the temperature is slower than the rate at RHIC [recall the $T = T_0(\tau_0/\tau)^{1/3}$]. This implies that even though the initial temperature is much higher than the temperature at RHIC, the enhancement factor may not be much different. With τ_0 fixed at 0.1 fm, we get

$$\frac{(dN_{\eta'}/dy)_f}{(dN_{\eta'}/dy)_{f_{\rm vac}}} \approx 2-3 \quad \text{(LHC)} \tag{3.4}$$

between $T_0 = 0.5$ GeV and $T_0 = 1.0$ GeV. The maximum enhancement factor 3 is reached at $T_0 = 0.6$ GeV.

At SPS, the enhancement factor is more sensitive to the initial temperature. Keeping $\tau_0 = 0.8$ fm [20], the ratio increases as the temperature increases within 0.2 GeV$\leqslant T_0 \leqslant$0.25 GeV:

$$0.3 \lesssim \frac{(dN_{\eta'}/dy)_f}{(dN_{\eta'}/dy)_{f_{\rm vac}}} \lesssim 1.1 \quad \text{(SPS)}. \tag{3.5}$$

Since η' decays to $\eta\pi\pi$ in 65% of the time, one may ask if this SPS result is compatible with the η multiplicity measurement by WA80 and the low mass dilepton spectrum measured by CERES. Thermal ratio of η' and η within the Bjorken scenario is 17%. Therefore one would expect that about 11% of η comes from η' decay. Doubling that would indicate about 10% increase in the η multiplicity. However, at present the experimental uncertainty is bigger than 10% [22,23].

More detailed information than the yield can be obtained in the transverse momentum distribution shown in Fig. 3. There is a clear difference between our calculation and the thermal distribution. As one can see, the dependence of the solution Eq. (2.16) on T_0 and τ_0 is nontrivial. Since the simple 1D model we employ does not take into account the transverse flow, the slope parameter of the p_T spectra in Fig. 3 should be taken as qualitative estimates rather than quantitative predictions.

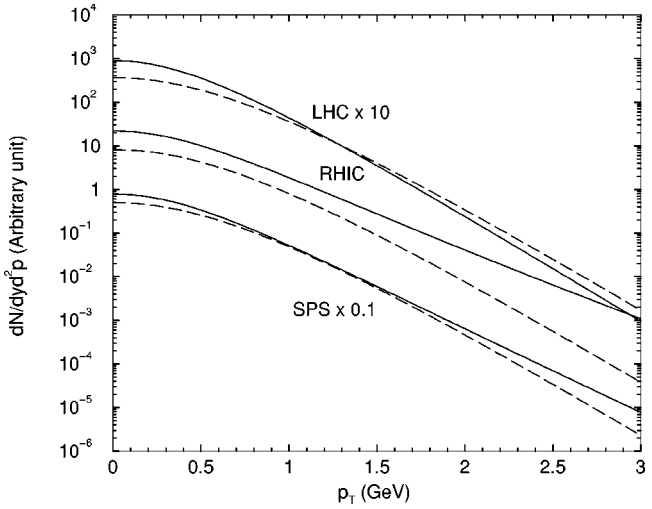

FIG. 3. The transverse momentum spectrum of η' calculated with the solution Eq. (2.16) (solid line) and the thermal $e^{-E_P^0 \cosh \eta/T_c}$ (dashed line) where E_P^0 is calculated with the vacuum η' mass. For the top two lines, we used $T_0=1$ GeV and $\tau_0=0.1$ fm estimated for LHC in Ref. [21]. SPS and RHIC parameters are $T_0=0.257$ GeV, $T_0=0.334$ GeV and $\tau_0=0.8$ fm, $\tau_0=0.6$ fm, respectively [20]. Transverse expansion is not taken into account.

IV. DISCUSSION AND CONCLUSION

In this paper, we calculated the yield and the momentum spectrum of the flavor singlet η' mesons produced by the fusion of thermal gluons. It is shown above that at RHIC and LHC, there is a significant enhancement in η' yield. Furthermore, the p_T spectrum of η' shows an interesting deviation from the M_T scaling. The onset of the deviation from the naive M_T scaling contains information on the initial conditions such as the initial temperature and the thermalization time. This may be feasible since η' has a long lifetime and a long mean free path.

Further implication of our result includes the low-mass dilepton enhancement. The branching ratio of $\eta' \to \eta\pi\pi$ is 65%. A large number of η' results in a sizable increase in η multiplicity which in turn gives rise to the η Dalitz peak in the dilepton invariant mass spectrum. At SPS, the enhancement is not significant enough to be noticed. But at RHIC and LHC, there can be a substantial increase of the peak. Another observable where η' enhancement plays a role is the HBT correlation. As shown in Ref. [24], enhanced η' production reduces the strength of the HBT correlation at small p_T.

The above conclusions are based on the effective $gg\eta'$ vertex deduced by Atwood and Soni, the kinetic (Boltzmann) equation, and also the following assumptions.

(i) The gluons are locally thermalized and follow the hydrodynamic evolution.

(ii) The strength of $gg\eta'$ vertex is independent of the temperature.

(iii) The mass of η' involved in this process is lower than the vacuum value since only the *s* quark loop is involved in the anomalous coupling.

(iv) Kinetic equation is valid in this regime.

As to the validity of the hydrodynamics, the measurements of the elliptic flow indicate the existence of collective motion. Whether this implies thermal and chemical equilibrium is not entirely certain. Since our result indicates that the η' density is proportional to the square of the gluon density, the measured η' dN/dy must reflect the underlying gluon distribution be it thermal or the gluon x distribution function. For instance, if the plasma is gluon dominated right up to the hadronization, then one should see even more η' than what we have estimated.

One may also question the validity of the 1D expansion model we employed. The full 3D calculation with a realistic equation of state is clearly out of the scope of this paper. However, our main results should be robust since faster falling temperature makes the η' distribution overshoot even more.

The temperature dependence of the $gg\eta'$ vertex and properties of η' itself are at present not fully understood. In this study, we made simple assumptions to make a progress. As we argued in the Introduction, the strength of $gg\eta'$ vertex will not vanish as the strength of $\pi^0\gamma\gamma$ vertex does at T_c. If one accepts the rough estimate, Eq. (1.5) at face value, then the strength of the $gg\eta'$ coupling could even be larger than H_0. The exact temperature dependence of the vertex, however, has yet to be worked out. The crucial question is then, what exactly is the relation between H_0 and $M_{\eta'}$ as a function of temperature? High-statistics measurement of η' spectrum can potentially answer this question by employing the ideas developed in this paper.

The kinetic equation description is valid when the mean free path is much larger than any other length scale. This is certainly the case. The mean free time of the η' is longer than 4 fm. The dense medium at $T=300$ MeV has a much smaller interparticle distance. The effect of inclusion of other processes such as $q\bar{q} \to \eta'$ can be roughly estimated by raising the value of H_0. In our calculation, this leads to more η' production by shortening $t_{\rm rel}$.

In summary, we have shown that η' is a good probe of the gluons density using the recently proposed $gg\eta'$ effective vertex. Other application along the same idea includes the investigation of the in-medium properties of η' and its possible link to the fate of the axial anomaly in a quark-gluon plasma. It will be also interesting to study formation of η' within gluon jets. These and other aspects are currently under investigation.

ACKNOWLEDGMENTS

The author is grateful to S. Pratt, J. Jalilian-Marian, L. McLerran, A. Soni, C. Gale, D. Kharzeev, and S. Bass for helpful suggestions and discussions. This work was supported in part by the Natural Sciences and Engineering Research Council of Canada and by le Fonds pour la Formation de Chercheurs et l'Aide à la Recherche du Québec.

APPENDIX A: REAL PART OF THE η' SELF-ENERGY IN THERMAL GLUONS

The Feynman diagrams for the one-loop retarded self-energy of the η' in equilibrium are given in Fig. 1. These

can be calculated in many ways. In this paper, we adopt the set of Feynman rules derived in Ref. [25]. The diagrams then corresponds to the expressions

$$\Sigma_a(P)=\frac{-i}{2}\int\frac{d^4p}{(2\pi)^4}\frac{d^4q}{(2\pi)^4}(2\pi)^4\delta(p+q-P)\times[\mathrm{Tr}\,M(p,q)^2]G(p)G(q) \tag{A1}$$

and

$$\Sigma_b(P)=\frac{-i}{2}\int\frac{d^4p}{(2\pi)^4}\frac{d^4q}{(2\pi)^4}(2\pi)^4\delta(p+q-P)\times[\mathrm{Tr}\,M(p,q)^2]\Delta_+(p)\Delta_+(q), \tag{A2}$$

where

$$G(p)=\frac{i}{p^2+i\epsilon}+n_{BE}(p)2\pi\delta(p^2) \tag{A3}$$

and

$$\Delta_+(p)=\theta(p^0)2\pi\delta(p^2)+n_{BE}(p^0)2\pi\delta(p^2). \tag{A4}$$

The prefactor 1/2 comes from the fact that the two intermediate gluons are identical. Using these propagators, it is clear that the real part of the self-energy comes only from the diagram (a). Hence we concentrate on evaluation of (a) from now on.

First, we evaluate the vertex trace

$$\begin{aligned}(\mathrm{Tr}\,M(p,q)^2)&=\sum_{ab}\delta^{ab}\sum_{\lambda,\gamma}M^*_{\lambda\gamma}M_{\lambda\gamma}\\&=8H_0^2\epsilon_{\alpha\beta\mu\nu}\epsilon^{\alpha\beta\rho\sigma}p^\mu q^\nu p_\rho q_\sigma\\&=16H_0^2[(p\cdot q)^2-p^2q^2]\end{aligned} \tag{A5}$$

using the identities

$$\sum_\lambda(\epsilon_p^\alpha)^*_\lambda(\epsilon_p^\zeta)_\lambda=-g^{\alpha\zeta}+ap^\alpha p^\zeta \tag{A6}$$

and

$$\epsilon_{\alpha\beta\mu\nu}\epsilon^{\alpha\beta\rho\sigma}=2(g^\mu_\sigma g^\nu_\rho-g^\mu_\rho g^\nu_\sigma). \tag{A7}$$

The $ap^\alpha p^\zeta$ term does not contribute due to the antisymmetric property of $\epsilon_{\alpha\beta\mu\nu}$. Then

$$\begin{aligned}\Sigma_a(P)&=-8iH_0^2\int\frac{d^4p}{(2\pi)^4}\frac{d^4q}{(2\pi)^4}(2\pi)^4\delta(p+q-P)\times[(p\cdot q)^2-p^2q^2]G(p)G(q)\\&=-8iH_0^2\int\frac{d^4p}{(2\pi)^4}\{[p\cdot(P-p)]^2-p^2(P-p)^2\}G(p)G(P-p).\end{aligned} \tag{A8}$$

The zero-temperature part of this diagram is badly divergent. In view of the effective theory nature of this vertex, we will simply drop the zero-temperature part in this calculation. The thermal part can be separated into two parts,

$$\Sigma_a(P)=\Sigma_{a,1}(P)+\Sigma_{a,2}(P), \tag{A9}$$

where

$$\Sigma_{a,1}(P)=-16iH_0^2\int\frac{d^4p}{(2\pi)^4}(p\cdot P)^2\times\frac{i}{M^2-2P\cdot p+i\epsilon}n(p)2\pi\delta(p^2) \tag{A10}$$

and

$$\Sigma_{a,2}(P)=-8iH_0^2\int\frac{d^4p}{(2\pi)^4}(p\cdot P)^2n(E_{P-p})\times2\pi\delta(M^2-2P\cdot p)n(p)2\pi\delta(p^2), \tag{A11}$$

and we used the on-shell conditions $p^2=0$ and $P^2=M^2$.

The real part of the self-energy comes only from $\Sigma_{a,1}(P)$:

$$\begin{aligned}\mathrm{Re}\,\Sigma_{\mathrm{ret}}(P)&=\mathrm{Re}\,\Sigma_{a,1}(P)\\&=16H_0^2\int\frac{d^4p}{(2\pi)^4}(p\cdot P)^2\mathrm{PP}\times\frac{1}{M^2-2P\cdot p}n(p)2\pi\delta(p^2)\\&=-4H_0^2M^2\int\frac{d^4p}{(2\pi)^4}n(p)2\pi\delta(p^2)+4H_0^2M^4\int\frac{d^4p}{(2\pi)^4}\mathrm{PP}\frac{1}{M^2-2P\cdot p}\times n(p)2\pi\delta(p^2),\end{aligned} \tag{A12}$$

where PP signifies the principal part.

For simplicity, we orient $P^\mu=(E_P,0,0,P)$ and approximate the Bose-Einstein factor by a Boltzmann factor

$$n(p)\approx e^{-p/T}. \tag{A13}$$

Then

$$\begin{aligned}\mathrm{Re}\,\Sigma(P)&\approx-4H_0^2M^2\frac{1}{(2\pi)^2}\int dppe^{-|p|/T}+4H_0^2M^4\int\frac{d^4p}{(2\pi)^4}\mathrm{PP}\frac{1}{M^2-2P\cdot p}e^{-|p|/T}2\pi\delta(p^2)\\&=-4H_0^2M^2\frac{T^2}{(2\pi)^2}\times\left[1-+\frac{M^2}{4PT^2}\int dpe^{-p/T}\left\{\ln\left|\frac{M^2-2Ep+2Pp}{M^2-2Ep-2Pp}\right|+\ln\left|\frac{M^2+2Ep+2Pp}{M^2+2Ep-2Pp}\right|\right\}\right].\end{aligned} \tag{A14}$$

The result can be expressed in terms of the exponential integral functions

$$\mathrm{Re}\,\Sigma_{\mathrm{ret}}(P)=-M^2\frac{4H_0^2T^2}{(2\pi)^2}\left(1-\frac{M^2}{4PT}A(P)\right), \quad \text{(A15)}$$

where

$$A(P)=M^2e^{-(P+E_P)/2T}\left[-e^{E_P/T}\mathrm{Ei}\left(\frac{P-E_P}{2T}\right)+e^{P/T}\mathrm{Ei}\left(\frac{-P+E_P}{2T}\right)+e^{(P+E_P)/T}\mathrm{Ei}\left(\frac{-(P+E_P)}{2T}\right)-\mathrm{Ei}\left(\frac{P+E_P}{2T}\right)\right]. \quad \text{(A16)}$$

Numerically, between $T=0.17$ GeV and $T=1.0$ GeV, the second term is important only near $P=0$. Therefore we approximate the above with

$$\mathrm{Re}\,\Sigma_{\mathrm{ret}}(P)\approx\Sigma_{\mathrm{ret}}(P=0)=-M^2\frac{4H_0^2T^2}{(2\pi)^2}\times\left(1-\frac{M^2}{4T}[e^{M/2T}\mathrm{Ei}(-M/2T)+e^{-M/2T}\mathrm{Ei}(M/2T)]\right). \quad \text{(A17)}$$

We can self-consistently determine M by solving the following equation for M with $M_0=0.7$ GeV:

$$M^2=M_0^2+\mathrm{Re}\,\Sigma_{\mathrm{ret}}(0). \quad \text{(A18)}$$

Numerically solution of this equation indicates that $M(T)$ is a slow varying function of T. At $T=0.17$ GeV, $M(T)=0.7$ GeV is indistinguishable from M_0. Even at $T=0.5$ GeV, $M(T)=0.68$ GeV. Only around $T=1$ GeV, $M(T)=0.64$ GeV is appreciably different from M_0. However, at this temperature, our Boltzmann approximation is no longer appropriate. We can ignore the temperature dependence of the η' mass for our estimates.

APPENDIX B: TWO-BODY THERMAL PHASE SPACE

We start from the expression

$$\Gamma_2(P)=\int\frac{d^3p}{(2\pi)^3 2p}\frac{d^3q}{(2\pi)^3 2q}(2\pi)^4\times\delta(p+q-P)f_g(p)f_g(q). \quad \text{(B1)}$$

Carrying out the d^3p integral and the q angle integral yields

$$\Gamma_2(P)=\frac{1}{4}\int\frac{d^3q}{(2\pi)^3q|\mathbf{P}-\mathbf{q}|}(2\pi)\,\delta(|\mathbf{P}-\mathbf{q}|+q-E_P)\times f_g(|\mathbf{P}-\mathbf{q}|)f_g(q)=\frac{1}{4}\frac{1}{2\pi}\frac{1}{|\mathbf{P}|}\int_{q_{\min}}^{q_{\max}}dq\,f_g(E_P-q)f_g(q), \quad \text{(B2)}$$

where

$$q_{\min}=\frac{M^2}{2(E_P+P)} \quad \text{(B3)}$$

and

$$q_{\max}=\frac{M^2}{2(E_P-P)}. \quad \text{(B4)}$$

Using the Bose-Einstein functions for f, we get

$$\Gamma_2(P)=f_{BE}(E_P)\frac{T}{8\pi|\mathbf{P}|}[\ln(e^{q_{\max}/T}-1)-\ln(e^{q_{\min}/T}-1)+\ln(e^{E_P/T}-e^{q_{\min}/T})-\ln(e^{E_P/T}-e^{q_{\max}/T})]. \quad \text{(B5)}$$

In $T\to 0$ limit, we recover the Boltzmann result

$$\Gamma_2(P)=\frac{1}{8\pi}e^{-E_P/T}. \quad \text{(B6)}$$

[1] A. A. Belavin, A. M. Polyakov, A. S. Shvarts, and Y. S. Tyupkin, Phys. Lett. **59B**, 85 (1975).
[2] E. Witten, Nucl. Phys. **B156**, 269 (1979).
[3] G. Veneziano, Nucl. Phys. **B159**, 213 (1979).
[4] G. 't Hooft, Phys. Rev. Lett. **37**, 8 (1976).
[5] J. Kapusta, D. Kharzeev, and L. McLerran, Phys. Rev. D **53**, 5028 (1996).
[6] A. L. Kagan and A. A. Petrov, "η' production in B decays: Standard model vs. new physics," hep-ph/9707354.
[7] D. Atwood and A. Soni, Phys. Lett. B **405**, 150 (1997).
[8] T. Muta and M. Yang, Phys. Rev. D **61**, 054007 (2000).
[9] A. Ali, J. Chay, C. Greub, and P. Ko, Phys. Lett. B **424**, 161 (1998).
[10] W. Hou and B. Tseng, Phys. Rev. Lett. **80**, 434 (1998).
[11] P. H. Damgaard, H. B. Nielsen, and R. Sollacher, Nucl. Phys. **B414**, 541 (1994).
[12] T. Muta and M. Z. Yang, "→ eta X/s," hep-ph/9902275
[13] R. D. Pisarski, T. L. Trueman, and M. H. Tytgat, Phys. Rev. D **56**, 7077 (1997).
[14] S. P. Kumar, D. Boyanovsky, H. J. de Vega, and R. Holman, Phys. Rev. D **61**, 065002 (2000).
[15] H. Itoyama and A. H. Mueller, Nucl. Phys. **B218**, 349 (1983).
[16] T. Schafer, Phys. Lett. B **389**, 445 (1996).
[17] P. Elmfors, Nucl. Phys. **B487**, 207 (1997).
[18] S. Jeon, Phys. Rev. D **52**, 3591 (1995).
[19] S. Jeon and L. G. Yaffe, Phys. Rev. D **53**, 5799 (1996).
[20] P. F. Kolb, P. Huovinen, U. Heinz, and H. Heiselberg, Phys. Lett. B **500**, 232 (2001).
[21] K. J. Eskola, K. Kajantie, P. V. Ruuskanen, and K. Tuominen, Nucl. Phys. **B570**, 379 (2000).

[22] WA80 Collaboration, A. Lebedev *et al.*, Nucl. Phys. **A566**, 355C (1994).
[23] WA80 Collaboration, R. Albrecht *et al.*, Phys. Lett. B **361**, 14 (1995).
[24] S. E. Vance, T. Csorgo, and D. Kharzeev, Phys. Rev. Lett. **81**, 2205 (1998).
[25] S. Jeon and P. J. Ellis, Phys. Rev. D **58**, 045013 (1998).